15 April 2000

ELSEVIER

Optics Communications 177 (2000) 47–55

OPTICS COMMUNICATIONS

www.elsevier.com/locate/optcom

Optimisation of depth-graded multilayer coatings for broadband reflectivity in the soft X-ray and EUV regions

Alan G. Michette [a,*], Zhanshan Wang [a,b]

[a] *Department of Physics, King's College London, Strand, London, WC2R 2LS, UK*

[b] *State Key Laboratory of Applied Optics, Changchun Institute of Optics and Fine Mechanics, Chinese Academy of Sciences, P.O. Box 1024, Changchun 130022, China*

Received 30 November 1999; received in revised form 21 February 2000; accepted 22 February 2000

Abstract

A systematic method which allows the optimum thickness of each layer in a depth-graded multilayer coating to be determined is described. This enables specific reflectivity responses over broad wavelength bands in the soft X-ray and EUV regions to be calculated. The method is applied to the design of some depth-graded molybdenum/silicon multilayers for the wavelength range 13–19 nm, with average normal incidence reflectivities of about 13% in this range, but it is generally applicable for other material pairs and wavelength ranges. In addition, the effects of layer thickness errors on the performance of depth-graded multilayers can be simulated. The model gives better results than those based on power law variation of the layer thicknesses.

PACS: 41.50; 78.66

Keywords: Depth-graded multilayer mirrors; Soft X-ray and EUV optics; Broadband X-ray optics

1. Introduction

Remarkable progress has been made in the field of normal incidence soft X-ray and extreme ultraviolet (EUV) multilayer mirrors in recent years [1,2]. In most cases the multilayers have constant bilayer thicknesses and a peak reflectivity at a given wavelength and incidence angle. In the soft X-ray and EUV region, the real parts of the refractive indices for all materials have small deviations, δ, from unity, and thus coherent addition of reflections from many layers in a constant bilayer thickness multilayer mirror is required to reflect a significant percentage of an incident beam at a given wavelength and angle. This produces a narrow bandpass and high peak reflectivity. However, there are some applications that require relatively broad band spectral throughout. These applications include soft X-ray multilayer coated imaging optics [3,4], for example as used in EUV lithography, which need maximum integrated reflectivity (possibly convolved with the source emission spectrum), spectroscopies with multilayer coated gratings [5] and multilayer coated col-

* Corresponding author. Tel.: +44-20-7848-2811; fax: +44-20-7848-2121; e-mail: alan.michette@kcl.ac.uk

0030-4018/00/$ - see front matter
PII: S0030-4018(00)00589-7

lecting optics [6], where the wavelength range is defined by the spectral bandpass of the multilayer coatings.

An early suggestion leading to increased angular and wavelength responses of multilayer mirrors in soft X-ray region was made by Nagel et al. [7] using depth-graded multilayer coatings. Meekins et al. [8] designed some depth-graded multilayer coatings for the soft X-ray and EUV region which increased the wavelength bandpass but decreased the peak reflectivity. Vernon et al. [9] fabricated depth-graded Mo/Si multilayer coatings with bilayer thicknesses linearly decreasing from the top of the multilayer structure to the substrate. Compared to constant period Mo/Si multilayers these depth-graded Mo/Si multilayer coatings had large wavelength bandpasses and small peak reflectivities. Seely et al. [10] also made depth-graded W/B_4C multilayer coatings with structures similar to those of Vernon. Recently there has been significant progress in depth-graded multilayer coatings for the hard X-ray region, providing broadband reflectivity at grazing incidence. Such mirrors can be used in a variety of applications including synchrotron and medical optics, and, in particular, for space-borne astronomical hard X-ray telescopes [11,12].

Other optimisation procedures have been discussed by Vidal et al. [13], Erko et al. [14] and Høghøj et al. [15]. In particular, Loevezijn et al. [16] have described an optimisation method that can be used to generate specified bandpasses for the soft X-ray range. The systematic method for optimising the design of broadband multilayer mirrors for the soft X-ray and EUV regions described here is similar to that of Loevezijn et al. [16] but has been applied more generally, to take into account, for example, interfacial roughness, layer thickness errors and non-sharp boundaries. The application of the method in optimising the throughput of a system (mirror reflectivity times source spectrum) will be addressed in a forthcoming paper.

In Section 2 of the present paper the optimisation technique is described, and in Section 3 it is applied to some Mo/Si depth-graded multilayers with specific performance requirements. The influences of roughness, layer thickness errors and non-sharp boundaries on the multilayer performance are discussed in Section 4. In the concluding section, a comparison is made with the power law approach of Joensen et al. [17]

2. Design of broadband multilayer mirrors for the soft X-ray and EUV range

The design of a broadband multilayer coating requires the choice of materials and layer thickness distribution to give a reflectivity as high as possible for the specified wavelength range and a given incidence angle. A multilayer usually contains alternating layers of high (h) and low (l) atomic number materials. For a depth-graded multilayer coating, it is natural to describe the multilayer in terms of bilayers, each consisting of two adjacent layers, with a jth bilayer thickness $d_j = d_{j\mathrm{h}} + d_{j\mathrm{l}}$ (n the rest of this paper, j is taken to increase from the top of the multilayer downwards). The range and distribution of bilayer thicknesses in a depth-graded multilayer coating are given by the Bragg equation and determine the bandpass. The refraction corrected Bragg equation [18] for a multilayer coating with constant bilayer thickness d, fractional thicknesses d_h and d_l, and complex refractive indices $n_\mathrm{h} = 1 - \delta_\mathrm{h} - \mathrm{i}\beta_\mathrm{h}$ and $n_\mathrm{l} = 1 - \delta_\mathrm{l} - \mathrm{i}\beta_\mathrm{l}$ is

$$m\lambda = 2d\sin\theta\left[1 - \frac{2(d_\mathrm{h}\delta_\mathrm{h} + d_\mathrm{l}\delta_\mathrm{l})}{\sin^2\theta}\right]^{1/2} \qquad (1)$$

where m the reflection order, λ is the wavelength, and θ is the grazing incidence angle. First-order ($m = 1$) reflection is usually used in the soft X-ray and EUV range, and the range of bilayer thicknesses required to reflect over the wavelength range $\lambda_{\min} - \lambda_{\max}$ for $m = 1$ can be estimated from

$$d_{\min} = \frac{\lambda_{\min}}{2\sin\theta}\left[1 - \frac{2(\delta_\mathrm{h}d_\mathrm{h} + \delta_\mathrm{l}d_\mathrm{l})}{\sin^2\theta}\right]^{-1/2} \qquad (2a)$$

$$d_{\max} = \frac{\lambda_{\max}}{2\sin\theta}\left[1 - \frac{2(\delta_\mathrm{h}d_\mathrm{h} + \delta_\mathrm{l}d_\mathrm{l})}{\sin^2\theta}\right]^{-1/2}. \qquad (2b)$$

The best material pairs for multilayer coatings are those that form smooth and compositionally abrupt interfaces and have high optical contrast and minimal absorption, i.e., the performance of a multilayer

is limited by the optical properties of the materials as well as by their physical and chemical properties [19]. In the range $\lambda \sim 12.5$–20 nm, molybdenum and silicon are a common pair of materials and they give excellent performance. This combination is used here in the design of some depth-graded multilayers for the wavelength range 13–19 nm.

The performance optimisation of depth-graded multilayers for various applications uses a process that judges a design based on its required performance in a given range of wavelength and incidence angle.

2.1. Merit function and thickness change

The performances of depth-graded soft X-ray and EUV multilayer coatings can be calculated numerically with reasonable precision using the well-known recursive methods based on the Fresnel formulae, so long as the thickness of each layer in the film is known. However, a major point of interest is the inverse problem, i.e., the calculation of the bilayer thicknesses which provide the best approximation to the required shape of the reflectivity curve as a function of wavelength range. From the mathematical point of view, this is a typical variational problem which can be solved by a suitable optimisation method, again recursively and based on the Fresnel equations. Nevertheless, it is necessary not only to optimise the shape of the reflectivity curve, but also to make the average reflectivity as high as possible. In addition, in the soft X-ray and EUV region, interfacial roughness can severely reduce the specular reflectivity of depth-graded multilayer coatings at normal incidence. Thus, the roughness must be included in the calculations. The simplest way to model the effects of roughness is to use the standard analysis based on the Debye model. Assuming that the mean position of a layer boundary is not altered by the roughness, the amplitude of the reflectivity at the jth interface is reduced by a factor

$$D_j = \exp\left[-\frac{1}{2}\left(\frac{4\pi\sigma_j \sin\theta_j}{\lambda_j}\right)^2\right] \tag{3}$$

where σ_j is the root mean square value of the effective roughness and θ_j is the grazing incidence angle. Unless indicated otherwise in the following, all calculations were done with $\sigma_j = 0.3$ nm.

In the method used, the thickness of each layer in the multilayer coating is changed randomly in a finite range according to

$$d = d_0(1 + AR) \tag{4}$$

where $R \in [-1,1]$ are random numbers uniformly distributed between -1 and 1 and A is a proportionality factor. A change which results in an improvement, according to a merit function defined below, is accepted by the computer program written to implement the method, otherwise it is rejected. The program uses optical constants determined from the atomic scattering factors available on the Internet [20].

In a similar fashion to many optimisation methods, a numerical measure (the merit function) is needed to minimise undesired features in the reflectivity response of depth-graded multilayer coatings, in order to ensure that the optimisation generates the most desirable structure. Many functional forms can be chosen for the merit function, each representing a particular desired reflectivity curve shape. Because of the complicated relationship between reflectivity and film thickness, optimisation of the merit function is accomplished by taking numerical derivatives and changing the film thickness according to Eq. (4). For example, the merit function can be defined in terms of the form of the reflectivity curve which gives the maximum integrated reflectivity in a desired wavelength range. Alternatively, the measure which gives an approximately constant reflectivity at the highest obtainable value over the required wavelength range can be chosen. Whatever merit function is used, the thickness of each layer is allowed to change during the optimisation process, but the number and composition of the layers do not change during the optimisation for the results presented here.

2.2. Initial thickness distribution

To optimise fully a multilayer for a given material pair and wavelength range is a lengthy process. This is because there are $2N$ variables for a multilayer coating with N bilayers and the computational complexity of the problem scales with N. The problem

can be made more tractable by inputting an original layer thickness distribution for a constant bilayer thickness, but even then there can be differences in the calculated optimum results caused by different initial values of d and γ (the ratio of the thicknesses of the high atomic material and the bilayer). Thus the choice of a suitable initial thickness distribution is important for obtaining a good result. During the optimisation, the results from a previous iteration of the layer thickness distribution or a linear change of thickness from bottom to top of the multilayer can be used for a renewed input condition. This eventually converges to the optimum result.

3. Optimised depth-graded multilayers

In this section the optimisation of the designs of depth-graded multilayers with specified performance requirements is described.

3.1. Depth-graded multilayer coatings with maximum integrated reflectivity

Soft X-ray and EUV optical systems such as telescopes, microscopes and lithography devices often require maximum integrated reflectivity in a given wavelength region to yield images with high efficiency. The merit function for optimising the depth-graded multilayer design is then

$$MF_k = \int_{\lambda_{\min}}^{\lambda_{\max}} R^k \, \mathrm{d}\lambda \tag{5}$$

where k is the number of multilayer coated optics in the system. During the optimisation, a layer thickness change which increases MF_k is retained, finally leading to an optimised layer thickness distribution. (This may not give the best final result since it does not allow escape from a local maximum. A method which prevents this will be described in a future paper.)

As an example of the optimisation, Fig. 1(a) shows the reflectivities of three Mo/Si depth-graded single ($k = 1$) normal incidence multilayers designed for the wavelength ranges 17–19 nm, 15–19 nm and 13–19 nm. These calculations demonstrate that the shape of the reflectivity curve for a smaller wavelength range is better. The layer thicknesses for the largest wavelength range are shown in Fig. 1(b); the thickness distribution shows some large oscillations, which are typical for depth-graded multilayers. In Fig. 2(a) the calculated curves for $k = 1, 2, 3$ for the wavelength range 16–19 nm are shown, showing that the curve changes shape and the width decreases as the number of mirrors increases. The layer thicknesses for $k = 3$ are shown in Fig. 2(b).

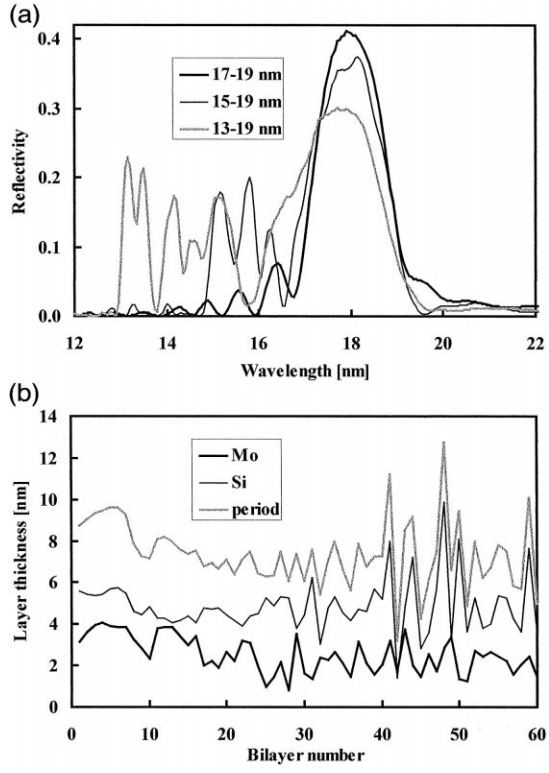

Fig. 1. (a) Calculated optimum normal incidence reflectivities versus wavelength of depth-graded Mo/Si multilayers for different wavelength ranges. The merit function to optimise the integrated reflectivity for one mirror was used, and an interfacial roughness of 0.3 nm was assumed. (b) Layer thicknesses versus the number of bilayers for the wavelength range 13–19 nm.

3.2. Depth-graded multilayers with flat reflectivity responses

For many applications, such as spectroscopy and lithography, large variability of reflectivity over the

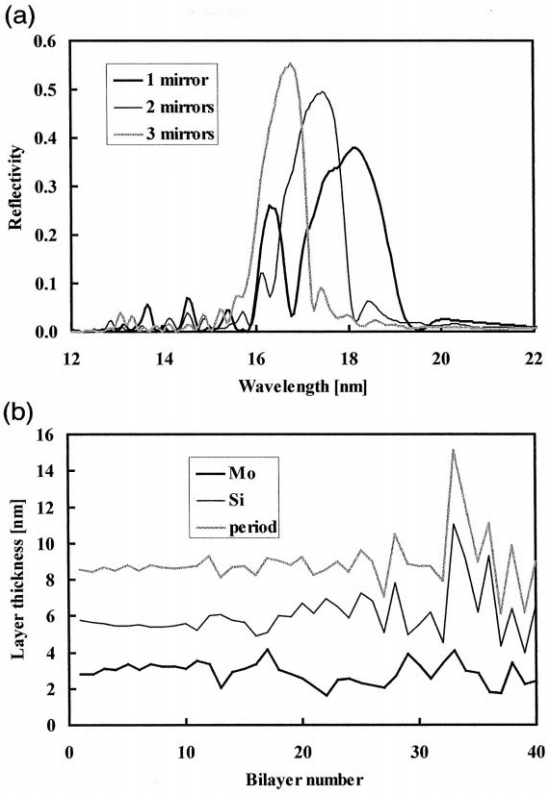

Fig. 2. (a) Calculated optimum normal incidence reflectivities versus wavelength of depth-graded Mo/Si multilayers for different merit functions (integrated reflectivity for 1, 2 and 3 mirrors) in the wavelength range 16–19 nm, and with 0.3 nm interfacial roughness. (b) Layer thicknesses versus the number of bilayers for 3 mirrors.

wavelength range may not be desirable. In this case merely maximising the integrated reflectivity is not the best approach. Instead, near uniform reflectivity in a defined wavelength range may be required. In order to design this kind of depth-graded multilayer, a possible merit function (for a single mirror) is

$$MF' = \int_{\lambda_{\min}}^{\lambda_{\max}} (R_\lambda - R_0)^2 \, \mathrm{d}\lambda \qquad (6)$$

where R_λ is the reflectivity of the multilayer coating at wavelength λ and R_0 is the required flat reflectivity value. Eq. (6) can readily be generalised for more than one mirror. In an optimisation the choice of R_0 is important, since choosing it too high will not allow a very flat response to be obtained. Fig. 3(a) shows the results for different R_0 (0.2, 0.25, 0.3) in the wavelength range 16–19 nm at normal incidence. The response clearly becomes less flat as R_0 increases, and the required value of reflectivity is not obtained; for $R_0 = (0.2, 0.25, 0.3)$ the average 16–19 nm reflectivities are 0.20, 0.225 and 0.23 respectively, with variations of $\pm 4\%$, $\pm 8\%$ and $\pm 14\%$. The layer thicknesses for $R_0 = 0.2$ are shown in Fig. 3(b).

Fig. 4(a) shows the reflectivities for the wavelength ranges 17–19 nm, 15–19 nm and 13–19 nm, with $R_0 = 0.28$, 0.19 and 0.14 respectively, at normal incidence. As would be expected, the response becomes less flat as the wavelength range increases, and also exhibits more oscillations. For the largest

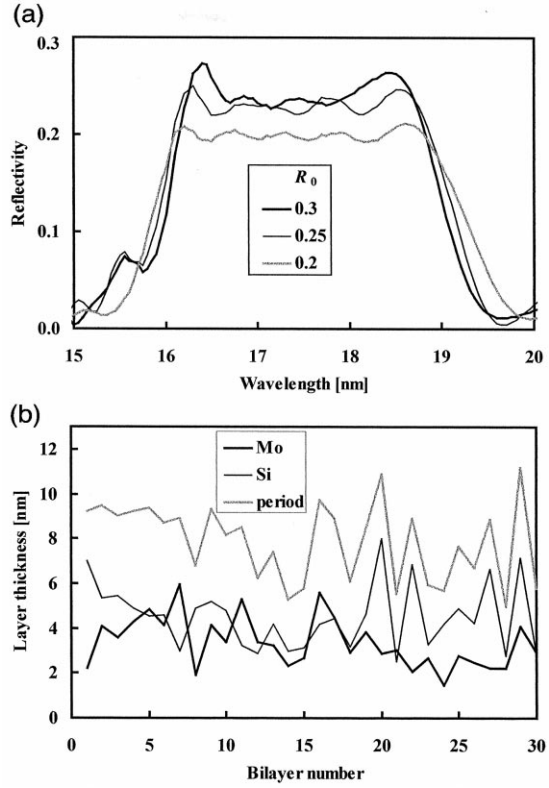

Fig. 3. (a) Calculated optimum reflectivity versus wavelength using the merit function to give a flat response with different target reflectivities, assuming 0.3 nm interfacial roughness. (b) Layer thicknesses of layers as a function of the bilayer number for a target reflectivities of 0.2.

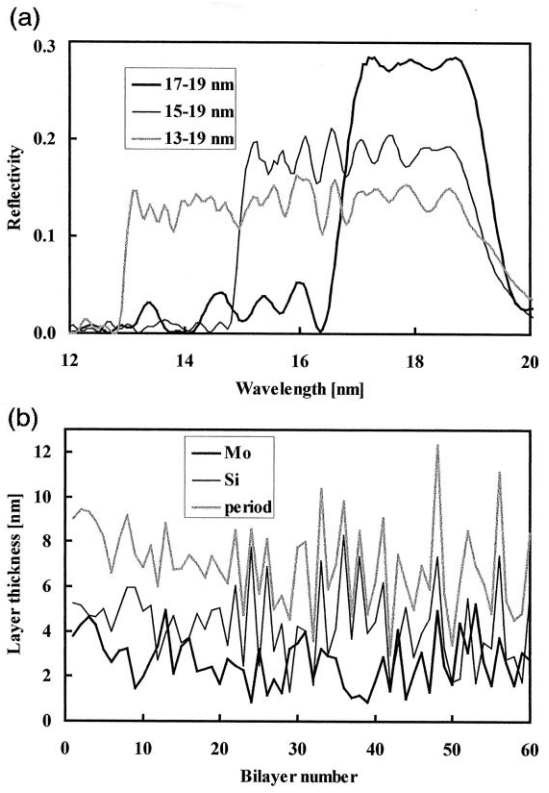

Fig. 4. (a) Calculated reflectivities of three depth-graded Mo/Si multilayers designed for flat responses in three different wavelength intervals. (b) Layer thickness distributions for the wavelength range 13–19 nm.

wavelength range the mean reflectivity is 0.135 with a variation of $\pm 10\%$; the layer thickness distribution is shown in Fig. 4(b).

4. Calculations including layer thickness errors

Many manufacturing inaccuracies, leading to layer thickness errors, can significantly affect the performance of a multilayer mirror. The errors can be localised, as in interfacial roughness, or global as in random or systematic incorrect layer boundary positions, or in non-sharp boundaries. It is important to incorporate these errors into the optimisation of a depth-graded multilayer, as they can influence the design parameters.

4.1. Roughness

Fig. 5 shows the calculated reflectivity of a Mo/Si depth-graded multilayer with a flat response in the wavelength region 13–19 nm at normal incidence without roughness and with roughnesses of 0.3, 0.6, and 0.9 nm. The reduction of the reflectivity is obvious as the roughness increases, although there is little reduction up to a roughness of 0.3 nm. For a roughness of 0.6 nm the mean reflectivity is reduced to 0.116 and the variation across the wavelength range increases to $\pm 11\%$, and for a roughness of 0.9 nm the corresponding values are 0.089 and $\pm 14\%$.

4.2. Systematic layer thickness errors

Permitted layer thickness errors in depth-graded multilayer coatings are very small. If the error is systematic, there is a fixed shift Δd of all layer thicknesses,

$$d_j = d_{j0} + \Delta d \tag{7}$$

where d_{j0} and d_j are the design and actual thicknesses of the jth layer. Fig. 6 shows the calculated reflectivity curves for a Mo/Si depth-graded multilayer designed for a flat response in the wavelength range 13–19 nm for layer thickness shifts of 0 and ± 0.2 nm. The curves show two effects, a shift in the wavelength range — negative (positive) for negative (positive) Δd — and increased oscillations. For the negative shift the mean reflectivity is reduced to

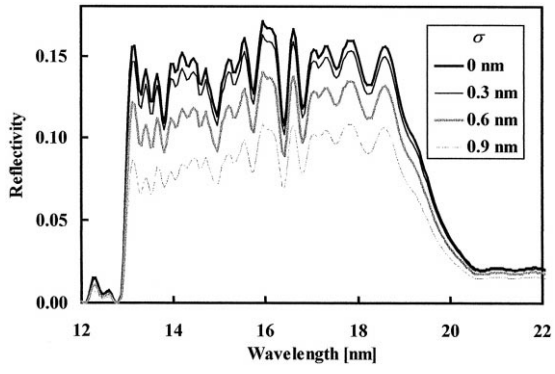

Fig. 5. The calculated reflectivities of Mo/Si depth-graded multilayers designed for flat responses in the wavelength range 13–19 nm, showing the effect of roughness.

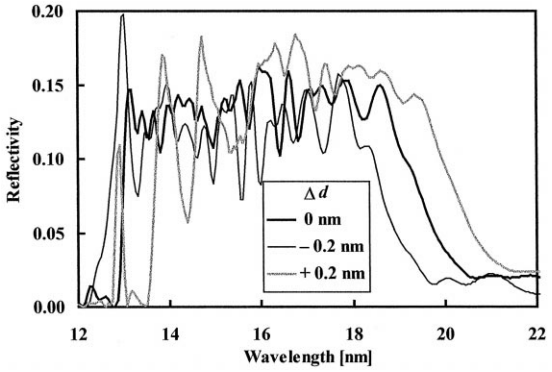

Fig. 6. The calculated reflectivities of Mo/Si depth-graded multilayers designed for flat responses in the wavelength range 13–19 nm, showing the effect of systematic boundary position errors.

0.116 and the variation over the wavelength range increases to $\pm 22\%$, and although for the positive shift the mean reflectivity is reduced only slightly to 0.130 the variation increases to $\pm 38\%$.

4.3. Random layer thickness errors

Random layer thickness errors can be modelled by

$$d_j = d_{j0}(1 + CR) \tag{8}$$

where C gives the largest fractional layer thickness error and $R \in [-1,1]$ are random numbers taken from a uniform distribution between -1 and 1 and. Fig. 7 shows the reflectivity curves for the average of 100 multilayers for $C = 0$–0.4. As C increases there is a slight broadening of the bandpass accompanied by a decrease in the average reflectivity. The results show that the influence of random layer thickness errors on the performances of depth-graded multilayers is not dramatic so long as the fractional thickness errors are kept below about 0.1 (corresponding to ~ 0.7 nm for the mirrors modelled here), for which the mean reflectivity is decreased to 0.130 and the variation across the range is also decreased to 8%.

4.4. Non-sharp boundaries

Interdiffusion of the layer materials into one another results in the sharp boundaries between layers assumed so far to be replaced by some form of transition layer. Four transition profiles have been suggested by Stearns [21], Gaussian, exponential and two linear profiles with different slopes. For the exponential profile, for example, the Fresnel reflection coefficients are multiplied by a factor $1/(1 + s^2\sigma^2)$ where, for normal incidence, $s = 4\pi/\lambda$ and σ characterises the width of the profile. Fig. 8 shows the reflectivity of the multilayer optimised for a flat response in the wavelength range 13–19 nm for an exponential transition profile with $\sigma = 0.3$ nm compared to the multilayer with sharp interfaces. The average 13–19 nm reflectivity is reduced from 0.135 to 0.130 (the target in each case was 0.14) while the variation increases from $\pm 10\%$ to $\pm 12.5\%$ (apart

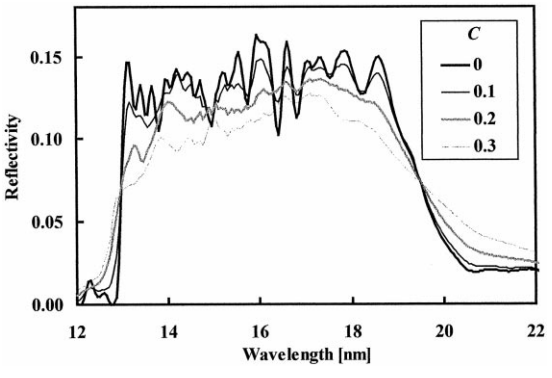

Fig. 7. The averaged calculated reflectivities of Mo/Si depth-graded multilayers designed for flat responses in the wavelength range 13–19 nm, showing the effect of random boundary position errors.

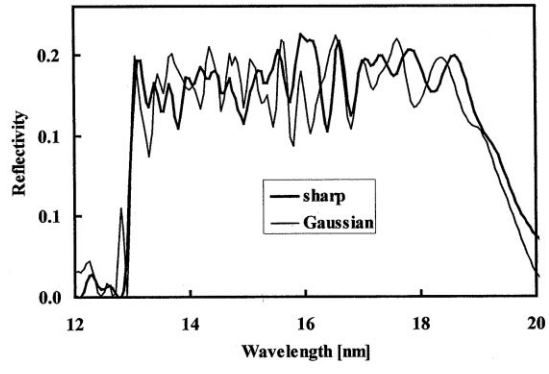

Fig. 8. The calculated reflectivities of Mo/Si depth-graded multilayers designed for flat responses in the wavelength range 13–19 nm, showing the effect of non-sharp boundaries.

from a large fluctuation close to 13 nm). The other transition profiles produce almost identical results.

5. Conclusions and discussion

Depth-graded multilayers with optimised layer thickness distributions will be useful in applications where a defined shape of the reflectivity curve in a given wavelength range is necessary. A systematic method of searching for optimum multilayer designs has been developed and used to design some multilayers for specific requirements. Two of the key factors in designing the multilayers are to define a suitable merit function to determine the performance and to specify suitable starting conditions for the optimisation. Various different merit functions have been specified, but others could equally well be chosen depending on the application.

Previous workers have suggested systematic variations in layer thicknesses to provide broadband reflectivity. The technique described in the current paper has been compared to the power law approach of Joensen et al. [17], in which the thickness d_j of the jth bilayer, counting from the top of the multilayer stack, is given by

$$d_j = \frac{a}{(b+j)^c} \tag{9}$$

where a, b (> -1) and c are the parameters which are varied, along with γ, the ratio of the molybdenum thickness to the bilayer thickness. The result of an optimisation for the 13–19 nm wavelength range with a target mean reflectivity of 0.14 is shown in Fig. 9(a), along with the result obtained using the method described in the current paper. Although the two models give similar mean reflectivities (0.135 for the current method, 0.131 for the power law model) and have the same variation of $\pm 10\%$ across the wavelength range, the power law model has a much longer tail at the long wavelength end of the range and also a less sharp cut-off at the short wavelength end. The values of the optimised power law parameters are $a = 10.4$ nm, $b = -0.87$, $c = 0.13$ and $\gamma = 0.43$, giving the bilayer thicknesses

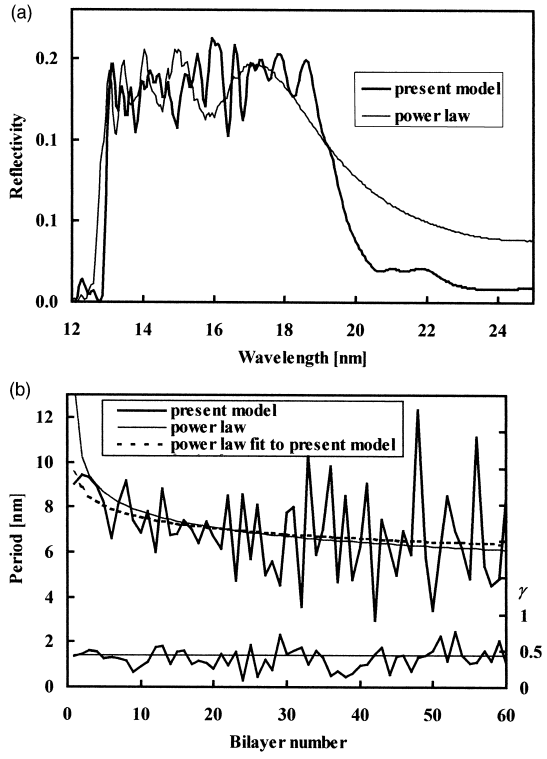

Fig. 9. (a) The calculated reflectivity of the Mo/Si depth-graded multilayer designed for flat responses in the wavelength range 13–19 nm compared to that calculated assuming a power law distribution of bilayer thicknesses. (b) The distribution of bilayer thicknesses in both cases. The lower two curves show the values of γ resulting from the calculations.

shown in Fig. 9(b). A power law fit to the bilayer thickness distribution obtained from the present model, also shown in Fig. 9(b), gives a curve lying close to that obtained from the power law model, suggesting that the power law result may be a good starting point for subsequent optimisation.

The influence of layer thickness errors on the performance of depth-graded multilayers has also been studied. It was found that roughness and systematic layer thickness errors significantly affect the performance, while random thickness errors and non-sharp boundaries have less effect.

Although the technique was applied to Mo/Si depth-graded multilayers working at normal incidence in the soft X-ray and EUV spectral region, it is completely general and can be used for other material pairs and wavelength ranges.

Acknowledgements

This study is financially supported in part by the National Natural Science Foundation of China for General Scientific Research, contract #69778026 to Z.W.

References

[1] E. Louis, A.E. Yakshin, P.C. Goerts, S. Abdali, E.L. Maas, R. Stuik, F. Bijkerk, D. Schmitz, F. Scholze, G. Ulm, M. Haidl, Proc. SPIE 3676 (1999) 844.
[2] C. Montcalm, B.T. Sullivan, H. Pepin, J.A. Dobrowolski, M. Sutton, Appl. Opt. 33 (1994) 2057.
[3] K. Murakami, T. Oshino, H. Nakamura, M. Ohtani, H. Nagata, Appl. Opt. 32 (1993) 7057.
[4] D.A. Tichenor, G.D. Kubiak, M.E. Malinowski, R.H. Stulen, S.J. Haney, K.W. Berger, L.A. Brown, R.R. Freeman, W.M. Mansfield, O.R. Wood II, D.M. Tennant, J.E. Bjorkholm, A.A. MacDowell, J. Bokor, T.E. Jewell, D.L. White, D.L. Windt, W.K. Waskiewicz, Opt. Lett. 16 (1990) 1557.
[5] T.W. Barbee Jr., G.E. Holland, C.N. Boyer, C.M. Brown, R.G. Cruddace, Appl. Opt. 32 (1993) 2422.
[6] E.N. Ragozin, N.N. Kolachevsky, M.M. Mitropolsky, V.A. Slemzin, N.N. Salashchenko, Proc. SPIE 2012 (1993) 209.
[7] D.J. Nagel, J.V. Gilfrich, T.W. Barbee Jr., Nucl. Instrum. Methods 195 (1982) 63.
[8] J.F. Meekins, R.G. Cruddace, H. Gursky, Appl. Opt. 26 (1987) 990.
[9] S.P. Vernon, D.G. Stearns, R.S. Rosen, Opt. Lett. 18 (1993) 672.
[10] J.F. Seely, M.P. Kowalski, W.R. Hunter, G. Gutman, Appl. Opt. 35 (1996) 4408.
[11] K. Yamashita, P.J. Serlemitsos, J. Tueller, S.D. Barthelmy, L.M. Bartlett, K.W. Chan, A. Furuzawa, N. Gehrels, K. Haga, H. Kunieda, P. Kurczynski, G. Lodha, N. Nakajo, N. Nakamura, Y. Namba, Y. Okajima, D. Palmer, A. Parsons, Y. Soong, S.M. Stahl, H. Takata, K. Tamura, Y. Tawara, B.J. Teegarden, Appl. Opt. 37 (1998) 8067.
[12] D.L. Windt, Appl. Phys. Lett. 74 (1999) 2890.
[13] B. Vidal, Z. Jiang, F. Samuel, Proc. SPIE 1738 (1992) 31.
[14] A. Erko, F. Schäfers, B. Vidal, A. Yakshin, U. Pietsch, W. Mahler, Rev. Sci. Instrum. 66 (1995) 4845.
[15] P. Høghøj, E. Ziegler, J. Susini, A.K. Freund, K.D. Joensen, P. Gorenstein, Physics of X-Ray Multilayer Structures, Optical Society of America, 1994, p. 142.
[16] P. van Loevezijn, R. Schlatmann, J. Verhoeven, B.A. van Tiggelen, E.M. Gullikson, Appl. Opt. 35 (1996) 3614.
[17] K.D. Joensen, P. Voutov, A. Szentgyorgyi, J. Roll, P. Gorenstein, P. Høghøj, F.E. Christensen, Appl. Opt. 34 (1995) 7935.
[18] T.W. Barbee Jr., Opt. Eng. 29 (1990) 711.
[19] C. Montcalm, P.A. Kearney, J.M. Slaughter, B.T. Sullivan, M. Chaker, H. Pepin, C.M. Falco, Appl. Opt. 35 (1996) 5134.
[20] B.L. Henke, E.M. Gullikson, J.C. Davis, At. Data Nucl. Data Tables 54 (1993) 181, see also http://cindy.lbl.gov/optical_constants.
[21] D.G. Stearns, J. Appl. Phys. 65 (1989) 491.